Time-Dependent Seismic Assessment of Typical Highway Bridges Subjected to Corrosion in Persian Gulf Zone

Afshin Kalantari[1] and Morteza Amooie[2]*

1. Assistant Professor, Structural Engineering Research Center (SERC), International Institute of Earthquake Engineering and Seismology (IIEES), Tehran, Iran,
* Corresponding Author; email: a.Kalantari@iiees.ac.ir
2. M.Sc. Student, Department of Civil Engineering, Islamic Azad University, South Tehran Branch, Tehran, Iran

Received: 26/05/2015
Accepted: 11/04/2016

ABSTRACT

In high seismic regions, such as Persian Gulf zone in Iran, corrosion of reinforcement and concrete deterioration can affect the seismic capacity of the structures and increase the vulnerability to the future seismic events. Although corrosion of reinforcement has the potential to affect all types of reinforced concrete structures, the highway bridges are vulnerable to more damage because of deicing salts, water splash or even seawater during their life cycle. The long-term corrosion process of a deteriorated typical RC highway bridge in Iran is analyzed as a function of time by using nonlinear static and dynamic analyses for seven earthquake ground motion records at three levels of intensity (0.3g, 0.5g and 0.75g). Three combined effects of corrosion (the loss of the cross sectional area of the reinforcement bars, decrease of the capacity of corroded reinforcing bars, and stiffness degradation of concrete cover resulting from reinforcement corrosion) were used in the time-dependent nonlinear analyses for six different time steps (i.e., non-corroded (t: 0), 10, 20, 30, 40, and 50 years) after corrosion initiation time. The results show that removing the concrete cover on bottom of columns has a greater impact on the structural capacity of the RC bridge than decreasing the rebar mechanical parameters.

Keywords:
Corrosion; RC highway bridge; Persian Gulf zone; Time-dependent nonlinear analyses; Seismic response

1. Introduction

Corrosion of the embedded bars in RC bridges is one of the primary causes of deterioration in bridge decks and piers [1]. Although corrosion of reinforcement has the potential to affect all types of reinforced concrete structures, the highway bridges in coastal regions are vulnerable to more damages because of deicing salts and seawater during their life cycle.

In the past, performance of RC bridges under a specific natural hazard such as an earthquake or wind or environmental stressor such as corrosion has been studied individually several times. Nevertheless, in real conditions, accurate assessment of bridge vulnerability demands the effects of those phenomena to be studied simultaneously. Corrosion of the embedded bars in RC bridges may cause intensive problems within the life cycle of the structure under earthquake events. Recently, response evaluation of corroded RC bridges under earthquakes has been studied in some researches (e.g. [2-4]).

Concrete structures are increasingly being deteriorated in Persian Gulf region, mainly due to the chloride-induced corrosion of the embedded

steel. Severity of this environment in which the average temperature exceeds more than 30°C and the relative humidity is about 70-90 % has made Persian Gulf one of the most aggressive environments in the world [5]. In high seismic regions, such as Persian Gulf zone in Iran, corrosion of reinforcement and concrete deterioration during their life cycle may weaken structures and make them more vulnerable to future earthquake hazards. Figure (1) shows examples of corroded RC pier exposed to seawater in Persian Gulf region.

When the RC bridges are located in coastal region, chloride ions existing in seawater penetrate the concrete cover, transport to the steel surface, destroy the protective passive layer, gradually increase and when the concentration on chloride ions at the surface of reinforcing bars reach a threshold value, corrosion is initiated. The effects of chloride-induced corrosion in RC columns of bridges and the effects of dynamic performance of structure are taken into account in this study.

In the present paper, computational approach is used to predict corrosion initiation time while considering experimental results obtained from Persian Gulf environmental conditions which are used to determine the main parameters in corrosion process, break this last sentence to a new sentence, it is a running phrase. It was assumed that the typical highway bridge studied in this article is located in Persian Gulf zone.

The time-dependent corrosion rate developed by Vu and Stewart [1] was used to compute the time-dependent corrosion effect parameters at various time steps in propagation period.

By increase of exposure time of a bridge to corrosive conditions, the degradation of reinforcement increases proportionally. This phenomenon results in spalling of the concrete and making the bars more slender. Structural weakening is calculated over the life of the bridge and new properties of RC member are updated at any given time.

In this study, in contrast to the previous studies (e.g. [2-4]), three combined effects of corrosion (the loss of the cross sectional area of the reinforcement bars, decrease of the capacity of corroded reinforcing bars, and stiffness degradation of concrete cover resulting from reinforcement corrosion) were used in the time-dependent nonlinear analyses of a corroded typical highway bridge while considering Persian Gulf environmental conditions.

To evaluate the structural capacity and seismic performance of deteriorated highway bridges, a typical RC highway bridge in Iran has been modeled. The design of these types of bridges was suggested by CODE No. 294 of the Management and Planning Organization of Iran [6].

When reinforcement bars get corroded, integrity and capacity are more likely to be reduced. In regions with seismic hazard, the strength reduction may become larger during an earthquake due to the loading demands. Therefore, recognizing time-variant risks shall help engineers and managers

Figure 1. Examples of corroded RC piers exposed to seawater in Persian Gulf zone, Boushehr

make more reasonable decisions considering optimization, inspection, maintenance and replacement of RC structures.

2. Service Life of Corroded Structures

The service life of concrete structures exposed to chloride ions can be presented by the modified version of Tuutti's two-stage model [7] shown in Figure (2).

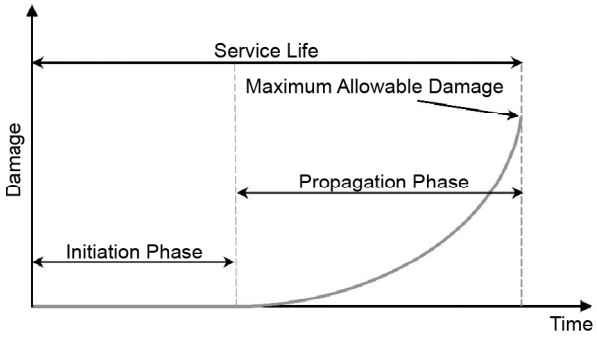

Figure 2. Service life model of a concrete member exposed to chloride ions.

2.1. Corrosion Initiation Phase

In this phase, chloride ions penetrate the concrete cover, transport to the steel surface, destroy the protective passive layer and accumulate over time until they reach the so-called "threshold level" to initiate corrosion [8].The duration of the initiation phase depends principally on the transport rate of the aggressive factors, the environmental conditions, design parameters (e.g. the concrete cover depth), and threshold level for corrosion initiation.

In numerous researches, it has been expressed that the primary mechanism for chloride transport through the concrete pore system is diffusion, such as ACI 365 [9], Choe [2-3] and Ghosh and Padgett [10].

Most diffusion models are based on the solution of the one-dimensional version of Fick's second law in a semi-infinite solid; which is expressed as Eq. (1):

$$\frac{\partial C}{\partial t} = D_c \frac{\partial^2 C}{\partial x^2} \tag{1}$$

where, C is chloride concentration at a distance x from the surface after the time t, and D_c is diffusion coefficient. In a commonly employed solution under the assumption of a constant diffusion coefficient, and boundary conditions specified as $C = C_s$ and the initial conditions specified as $C = 0$ for $x > 0$, $t = 0$, the chloride concentration C at depth x and time t is expressed as:

$$C_{(x,t)} = C_s\left[1 - erf\left(\frac{x}{2\sqrt{D_c t}}\right)\right] \tag{2}$$

where, $C_{(x,t)}$ is the chloride concentration at depth x after time t, erf is the error function, C_s is the chloride concentration on the concrete surface, D_c is diffusion coefficient (length^2/time), x is the distance from any point inside the concrete to the surface (length), and t is the time.

One of the major causes of chloride penetration is a condition to which concrete structure is subjected in marine environment [11]. Five exposure zones could be introduced including splash, tidal, submerged, soil and atmospheric zone according to the location of structural elements relative to seawater level. These five different exposure conditions are shown schematically in Figure (3).

Because the highway bridge studied in this article is located in Persian Gulf zone, experiment results in this area are used to determine the main parameters in corrosion process. The diffusion coefficient and the chloride concentration on the concrete surface are determined based on researches of Ghods et al. [11]. They have calculated D_c and C_s by curve fitting of the chloride profiles to Fick's second law of diffusion in different mixture properties and exposure conditions.

Values given for D_c and C_s in Persian Gulf's environmental conditions for a three months period are given in Tables (1) and (2).

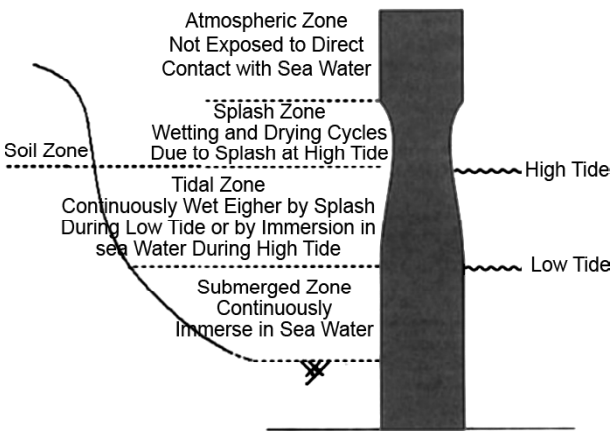

Figure 3. Schematically five different exposure conditions in Persian Gulf [11].

Table 1. Monthly average temperature [11].

Month	Temperature °C)
May	30.8
June	33.5
July	34.5

Table 2. Values of D_C and C_s after three months of exposure [11].

Zone	D_c(cm^2/yr)	C_s(% conc)
Atmosphere	0.262	0.051
Soil	0.382	0.033
Tidal	1.555	0.542
Submerged	1.372	0.570
Splash	1.523	0.948

The time to onset of chloride induced corrosion (T_i) occurs when the chloride concentration at the depth of the reinforcement (cover depth) reaches the critical chloride concentration, C_{cr} which depassivates the steel embedded in the concrete if sufficient moisture and oxygen are present. By setting $C_{(x,t)}$ equal to critical chloride threshold, C_{cr} the time to onset of corrosion is determined as follows:

$$T_i = \frac{x^2}{4D_c}\left[erf^{-1}\left(\frac{C_s - C_{cr}}{C_s}\right)\right]^{-2} \quad (3)$$

where, x is depth of concrete cover, D_c is chloride diffusion coefficient, C_{cr} is threshold level of chloride concentration that causes dissolution of the protective passive film around the reinforcement and initiates corrosion, C_s is the equilibrium chloride concentration at the concrete surface [12], and *erf* is Gaussian error function.

The corrosion initiation time depends on environmental exposure conditions. In this paper, it is assumed that the lower one third of all columns are exposed to corrosion in tidal conditions hence, the parameters describing the corrosion initiation of the RC columns adopted for the present study considering the Persian Gulf conditions are given in Table (3).

Due to above assumptions, the corrosion initiation time for the highway bridge studied in the present article and considering the corrosion in the lower one third of the columns caused by the tidal conditions, is 2.84 years. Determining corrosion initiation time in structures leads to anticipate desired life cycle for structures with respect to environmental conditions.

2.2. Corrosion Propagation Phase

After the corrosion initiation time, corrosion results in the formation of corrosion products which have been reported to be 4 to 6 times volume of metal iron [13]. In this process, the expansive corrosion products fill the concrete pores around the reinforcing steel and create internal tensile stresses on the concrete surrounding the corroding steel bar. This process continues until the volume of corrosion products reaches a level that causes the concrete cover to crack and spall as a usual consequence of corrosion of reinforcement bars in concrete.

In corrosion propagation phase in RC members, the performance level of structures decreases with time due to different effects. In this study, in contrast to previous studies, three combined effects of corrosion (the loss of the cross sectional area of the reinforcement bars, decrease of the capacity of corroded reinforcing bars, and stiffness degradation of concrete cover resulting from reinforcement corrosion) were used in the time-dependent non-linear analyses of corroded typical highway bridge considering Persian Gulf environmental conditions.

The effect of loss of bond between concrete and reinforcement is neglected in this study, because it has been reported that the reduction of bond has a negligible effect on bridge reliability in flexure for

Table 3. Variables affecting the corrosion.

Variable	Value	Unit
Chloride Diffusion Coefficient (D_c)	1.555	cm^2/yr
Surface Equilibrium Chloride Concentration (C_s)	0.542	% conc*
Critical Chloride Concentration (C_{cr})	0.050	% conc
Cover Depth (x)	5.000	cm

*% conc = Percent by Weight of Concrete

typical corrosion rates [1]. This is also supported by other researches Al-Sulaimani et al. [14], Ghandehari et al. [15] and Choe et al. [2] which show that the effect of corrosion on bond strength is negligible when a high percentage of confining transverse steel is used. In addition, because the bridge column example in this paper has a high transverse steel ratio in columns to confine the core concrete and ensure significant deformation before failure, the loss of bond strength is ignored in this work.

During the propagation phase, the corrosion rate is a significant parameter to evaluate the damage of corrosion effects. Different models have been developed to determine the corrosion rate. In some models it is assumed that the corrosion rate is constant (e.g. [16-18]) and in the other models assume that the corrosion rate is time variant [1], [19-22]. The purpose of this study is to evaluate time-dependent seismic performance hence, the time-dependent corrosion rate developed by *Vu* and Stewart [1] is used to compute the corrosion effects parameters over time. In this model, O_2 availability at the steel surface is assumed the governing factor. This model is suitable for regions with average relative humidity (RH) over 70% and temperature of 20°C like Iranian coast of Persian Gulf. For this environmental condition, corrosion rate up to one year after the end of the corrosion initiation phase was expressed empirically by Eq. (4):

$$i_{corr(1)} = \frac{37.8(1 - w/c)^{-1.64}}{d_c} \tag{4}$$

where $i_{corr(1)}$ is the corrosion rate at the start of corrosion propagation (μ A/cm^2), w/c represents the variable water-to-cement ratio, and d_c is cover depth (cm), which is the distance from the surface of steel bar to the surface of concrete structure. The corrosion rate at time t_p during the propagation phase is expressed as Eq. (5):

$$i_{corr}(t_p) = i_{corr(1)} 0.85 t_p^{-0.29} \tag{5}$$

where t_p is the time since corrosion initiation and $i_{corr(1)}$ is given by Eq. (4) for determining the corrosion rate at initiation of corrosion propagation phase [1].

3. Structural Deterioration Due to Corrosion

It is assumed that corrosion is generally uniform over the reinforcing steel surface. With this assumption, the diameter of the reinforcing bars will decrease with time and is a function of corrosion rate which is a time-dependent phenomenon. Therefore, the reduced diameter $D(t)$ of a corroding reinforcing bar at time t after corrosion initiation can be estimated using Faraday's Law as:

$$D(t) = D_0 - k_{corr} \int_0^t i_{corr}(t)\, dt \tag{6}$$

where $D(t)$ is the reduced diameter (length) of the reinforcing bar at some time, D_0 is the initial diameter of the reinforcing bar (length), $i_{corr}(t)$ is the corrosion rate (current/area^2), t is the time from corrosion initiation, and k_{corr} is the corrosion rate conversion factor which is 0.023 to convert corrosion rate from μ A/cm^2 to mm/year.

To predict the strength of deteriorated steel reinforcement, the experimental results reported by Due et al. [23-24] for estimating the residual strength of corroded bars were used in modeling of the corroded RC bridge. The empirical formula developed by Du et al. [23-24] to evaluate residual strength of corroded reinforcing bars embedded in concrete is used to calculate time-dependent loss of yield strength in corroded reinforcing bars.

$$f_y(t) = \left[1.00 - 0.005\, m(t)\right] f_{y0} \tag{7}$$

where $f_y(t)$ is the yield strength of corroded reinforcement at each time step; f_{y0} is the yield strength of non-corroded reinforcement; $m(t)$ is percentage of steel mass loss over time calculated from the consumed mass of steel per unit of length divided by original steel mass and t is time elapsed since the initiation of corrosion (years).

Concrete cover gets damaged because of reinforcement corrosion and can finally diminish after spalling off. When the stress at the boundary exceeds the tensile capacity of the concrete, the concrete cover will crack. Some attempts to develop a corrosion-cracking model have been made by various researchers. Some researchers have developed models to evaluate concrete cover degradation as a result of cracks, which are in turn induced by reinforcement cracks, using the mentioned approach.

In this study, models developed by Li et al. [25] and Zhong et al. [26] were used to assess the stiffness degradation of the concrete cover resulting from cracked concrete caused by corrosion of reinforcement as a function of the corrosion rate.

In these models, the concrete with embedded reinforcing bar is commonly modeled as a thick-wall cylinder, as shown schematically in Figure (4a). The concrete thick-walled cylinder subjected to internal pressure, radial pressure produced by principal bar ribs on surrounding concrete, exerted from the growth of corrosion products on the concrete at the interface between the steel bar and the surrounding concrete. In the concrete thick-walled cylinder model, D is the diameter of steel bar, a and b are the inner and outer radii of the thick-wall cylinder, d_c is the concrete cover depth, r is the distance from any point to the centroid of the cross section of the reinforcing bar, and d_0 is the original thickness of the annular layer of concrete pores prior to corrosion initiation at the interface between the steel bars and concrete. Once corrosion initiates, its products fill the pore band completely and form a ring of corrosion products forms, as shown in Figure (4b). The thickness of the corrosion products $d_s(t)$ can be determined from [20]:

$$d_s(t) = \frac{W_{rust}(t)}{\pi l(D+2d_0)}\left(\frac{1}{\rho_{rust}} - \frac{\alpha_{rust}}{\rho_{st}}\right) \quad (8)$$

where α_{rust} is a coefficient related to the type of corrosion product, ρ_{rust} is the density of the corrosion products, ρ_{st} is the density of the steel, l is the unit length (same length units as in ρ_{rust} and ρ_{st}), and $W_{rust}(t)$ is the mass of corrosion products per units length of rebar. To calculate $W_{rust}(t)$ as a function of the corrosion rate, Eq. (9) was proposed by Liu and Weyers [20]:

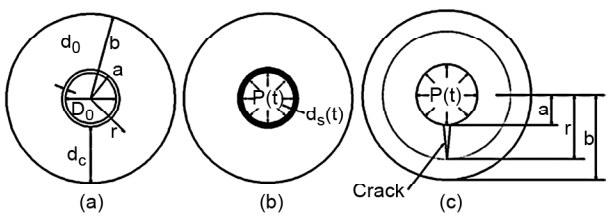

Figure 4. Schematic view of corrosion-induced concrete cracking process [25].

$$W_{rust}(t) = \left(2\int_0^t 0.105\,(1/\alpha_{rust})\pi D \times i_{corr}(t)\,dt\right)^{0.5} \quad (9)$$

When the stress at the steel-concrete interface exceeds the tensile strength of the concrete, the concrete will form cracks in the cover. Bazant and Planas [26] define the stiffness degradation factor (α) as:

$$\alpha = \frac{E_\theta}{E_{ef}} = \frac{\sigma/\varepsilon_\theta}{E_{ef}} \quad (10)$$

where σ is the cohesive stress, E_{ef} is the effective elastic modulus of concrete, and E_θ is the tangential elastic modulus of concrete for unloading. According to these authors, the total tangential strain ε_θ after cracking at location r and time t on a surface of the cohesive crack can be determined as:

$$\varepsilon_\theta = \varepsilon_\theta^e + \varepsilon_\theta^f \quad (11)$$

where ε_θ^e is elastic tangential strain and ε_θ^f is actual cracking strain. In addition, to calculate the cohesive stress, the following equation proposed by Li et al. [25] is used.

$$\sigma = \varphi(\varepsilon_\theta^f) = f_t e^{-\gamma\varepsilon_\theta^f} \quad (12)$$

where f_t is the tensile strength of concrete, and γ is a material constant. The thickness of the corrosion products, $d_s(t)$ is needed to calculate ε_θ and ε_θ^e (see the detailed algorithm for computing elastic tangential strain and actual cracking strain by Bazant and Planas [27] and Li et al. [25].

By substituting requirement parameters (Table 4) into Eq. (10), the stiffness degradation factor can be derived. Concrete stiffness degradation factor (α) is dependent on thickness of the corrosion product form, which is in turn a function of the mass of corrosion products per unit length of rebar. Besides, the mass of corrosion products per unit length of rebar can be calculated as a function of the corrosion rate, which is determined as a function of time. The predicted time-dependent mass of corrosion can predict the thickness of the corrosion product form as a function of the corrosion rate and type of corrosion products. Finally, the calculation of the time-dependent mass of corrosion products per unit length of rebar yields the time-dependent stiffness degradation factor for concrete cover.

Table 4. Values of basic variables for computing the stiffness degradation factor.

Variable	Value	Source
Thickness of Annular Layer of Concrete Pores (d_0)	0.0125 mm	Liu and Weyers (1998)
Corrosion Products Type Coefficient (α_{rust})*	0.570	Li et al. (2006)
Density of the Corrosion Products (ρ_{rust})	3600 kg/m^3	Liu and Weyers (1998)
Density of Steel (ρ_{st})	7850 kg/m^3	Liu and Weyers (1998)
Effective Elastic Modulus of Concrete (E_{ef})	21689.33 MPa	Present Study
Material Constant (γ)	1.3	Li et al. (2006)

*α_{rust} = Assume the composition of rust products is between $Fe(OH)_3$ and $Fe(OH)_2$, α_{rust} varies from 0.523 to 0.622.

Table 5. Values of the parameters for computing the effects of corrosion.

Time (year)*		0	10	20	30	40	50
Diameter (mm)	32	32.00	29.64	28.27	26.85	25.68	24.59
	20	20.00	17.64	16.27	14.85	13.68	12.59
	12	12.00	9.64	8.27	6.85	5.68	4.59
Yield Strength	$(M_{loss}/M_0)\times 100$	0.00	14.22	21.93	29.62	35.61	4096
	f_y/f_{y0}	1.00	0.93	0.89	0.85	0.83	0.80
Cover	α	1.00	0.45	0.05	0 (N.C.)**	0	0
Corrosion Rate ($\mu A/cm^2$)	i_{corr}	24.00	10.27	8.40	7.47	6.87	6.44

*year: After Corrosion Initiation **N.C.: No Concrete Cover

Considering the environmental condition in this article, a life cycle equal to 50 years after corrosion initiation time is assumed for the highway bridge under study in Persian Gulf zone. Hence, the Capacity of structure under study will be evaluated every 10 years after the corrosion initiation time. The parameters employed for structure to compute the effects of corrosion on structural and dynamic characteristics are shown in Table (5).

4. Numerical Study

4.1. Bridge Model

To evaluate the structural capacity and seismic performance of deteriorated highway bridges, a typical RC highway bridge in Iran has been modeled. The design of this type of bridges was suggested by CODE No. 294 of the Management and Planning Organization of Iran (MPO), which offers typical plans for similar bridges in different span lengths.

This model is a three-dimensional, three-span bridge with a bean-shaped column cross-section. An overview of the finite element model for the non-degraded bridge is presented herein for completion prior to describing the influence of corrosion on the bridge model. The present study focuses on the degradation of the RC columns in a corrosive environment and the effects of corrosion are not expected in the superstructure.

The deck spans between the columns include five girders with the same length. Total length of the bridge is 47.8 meters with a span width of 11.7 meters. A schematic view of the bridge under study is illustrated in Figure (5). Dimensions of the bridge studied in this paper corresponded to CODE No. 294 of the Management and Planning Organization of Iran (MPO) are summarized in Table (6).

The cover thickness presented in Table (6) represents the clear cover from the outer surface of the concrete to the edge of the transverse steel.

In this study, OpenSees software [28] is used to

Table 6. Principal dimensions of RC bridge under study.

Variable	Value
Total Length of the Bridge (m)	47.8
Span Width (m)	11.7
Column Height (m)	7.125
Distance between Columns (m)	3.25
Cover Depth (m)	0.05

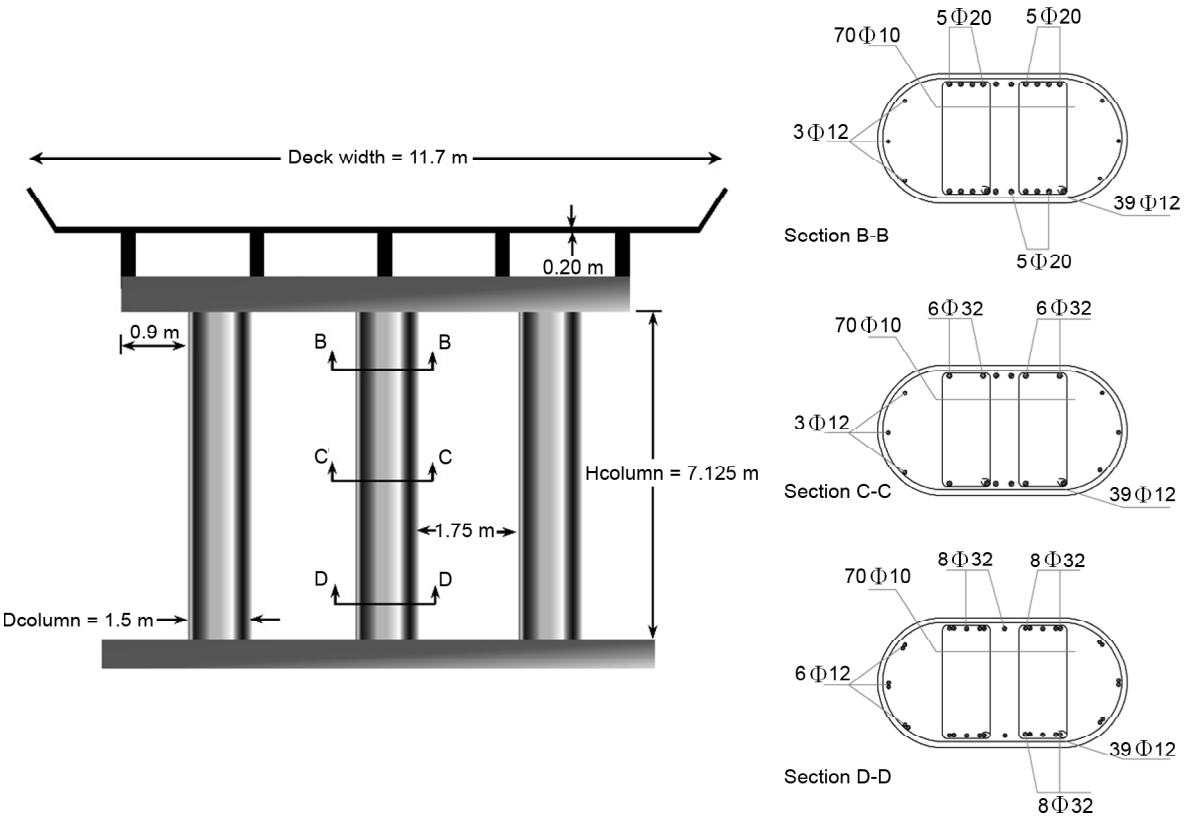

Figure 5. Schematic view of the bridge and section details.

analyze the structural response of the degraded structure after each ten-year interval. The OpenSees (Open System for Earthquake Engineering Simulation) software created by the University of California, Berkeley is used to build a finite element model of the RC bridge to accomplish static and dynamic analyses.

Figure (6) shows a simplified illustration of the OpenSees model that is used. The x-direction is referred to as the longitudinal direction, the y-direction is transverse, and the z-direction is vertical. There are six degrees of freedom for each node in the model: translation and rotation in the global *x*, *y*, and *z* directions. As shown in Figure (6), the columns, cap beams and decks are all subdivided into separate elements for the bridge model. Damping ratio of 0.045% and P-delta effect are considered in the model. The detailed assumptions made for the bridge components are discussed in the following sections.

4.2. Material Model

In this study, the analysis of confined corroded column of the highway bridge model was performed by using the uniaxial material model based on Kent-Scott-Park model with degrading linear unloading/reloading stiffness according to the work of Karsan-Jirsa [29].

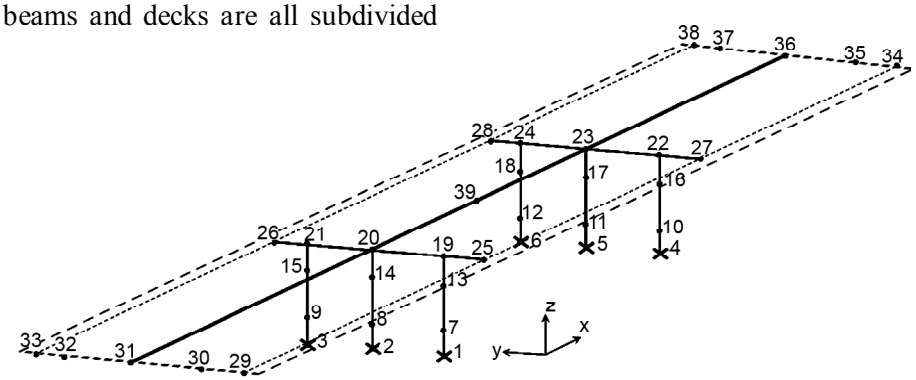

Figure 6. OpenSees bridge model representation.

The confined concrete (core) and unconfined concrete (cover) are defined using the Concrete01 material within OpenSees, which assumes that the concrete material has no tensile. For uncorroded materials, a strain of 0.002 for unconfined concrete under the maximum stress and a strain of 0.006 as a yield value are assumed. Confined concrete has a strain of 0.005 at a stress of 26.5 MPa and a strain of 0.05 at a stress of 25 MPa. As mentioned in the preceding section, the compressive strength of unconfined concrete (concrete cover) decreases over time causing the corrosion growth.

The concrete modulus of elasticity, E_c, is assumed to equal 21689.33 MPa for the normal weight concrete. In addition to concrete, mechanical properties of reinforcing bars in the analyses must also be modeled. The longitudinal reinforcements are modeled with a bi-linear stress-strain relation that accounts for strain hardening in OpenSees. The steel reinforcement is defined using the Steel01 material within OpenSees, which assumes linearly elastic behavior until the yield point is reached. Beyond yield, strain hardening is defined based on a ratio between the post-yield tangent and the initial elastic tangent stiffness. This model does not consider failure of bars in analyses. The yield strength is assumed to equal 400 MPa before corrosion initiation and the slope of strain hardening section is assumed 0.01 of the initial slope. As mentioned in the preceding section, the steel yield strength decreases over time causing the corrosion growth (Table 5).

4.3. Components Model

For the superstructure, the composite actions of the five continuous concrete girders and bridge deck are taken into account and modeled by linear-elastic beam-column elements placed at the centroid of the deck cross section. Total length of the bridge is 47.8 meters with a span width of 11.7 meters. Connections of deck to column are assumed rigid connection with no bearings. Since the columns are designed to nonlinear behavior, no nonlinear properties are assigned to the superstructure elements and they remain in the elastic range during applied forces.

To model the abutments, the rigid elements were used with a length equal to the deck width. Abutment at each end is subdivided into four equal elements. Connections of deck to abutments are assumed roller bearing.

The nonlinear tree-dimensional beam-column elements were used to model the bridge columns and cap beams. This element is force-based with distributed plasticity. The column is subdivided into three elements and specifications of these three elements that are different in properties are depicted in Figure (5).

Ignoring the SSI (Soil Structure Interaction), the lower node of the column is fixed and has no rotation and displacement. However, all other column nodes are free to move in any of the six degrees of freedom [30]. Concrete core, concrete cover, and steel reinforcement are used to create each column fiber sections. The fiber section is composed of some divisions in the concrete core. The number of fibers for both the cover and core are defined corresponding to details of Table (7). Besides, the steel reinforcement is considered by additional layers of bars in rectangular and semi-circle zone. An illustration of the column's fiber sections defined within OpenSees is shown in Figure (7).

Table 7. Column's fiber sections details.

	Rectangular Zone		Semi-Circle Zone	
	Y-Direction	Z-Direction	Radial	Sectorial
Core	10	10	8	6
Cover	10	2	2	6

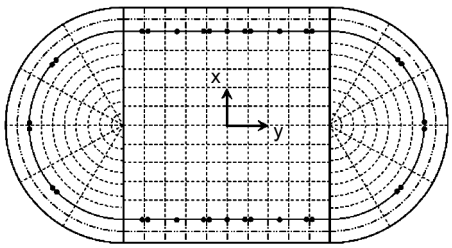

Figure 7. Illustration of the column's fiber sections.

5. Time-Dependent Nonlinear Analyses of Bridge

To evaluate the time-dependent response of the bridge, six models of this bridge were developed considering the effects of corrosion on the columns of the highway bridge during propagation period. Besides the pristine model of bridge, five models

correspondent to effects of corrosion at the time points of 10, 20, 30, 40 and 50 years were considered in the modeling process. It should also be mentioned that each of the time points are relative to the corrosion initiation time. Models related to the mentioned time points are constructed considering the effects of the correspondent corrosion in previous sections.

In this paper, to evaluate the capacity and performance of the typical highway bridge in Iran Highway Code, the nonlinear static and dynamic analysis are performed. Towards this goal, to estimate the remained capacity of bridge cases at different ages, the nonlinear static analysis (pushover) is employed. Then the natural periods of each six bridge cases are calculated with modal analysis and finally the nonlinear time history analysis is used to estimate the seismic response of each bridge at different ages.

Pushover curves for the bridge were obtained from the nonlinear static analyses and were developed for the bridge in different ages. The results of this analysis demonstrate the relationship between the total base shear in the columns and the relative lateral drift between the top and bottom of the column. The pushover curves for all cases are shown at Figure (8).

As shown in Figure (8), there is an obvious deterioration in the section capacity due to corrosion during corrosion propagation period. Additionally, a decrease of the yielding points and initial stiffness of the bridge is resulted from pushover analyses. The total base shear values change as the drift increases; therefore, reduction percent relative to pristine model at 1% to 6% relative lateral drift are presented in Table (8) to compare the corrosion damage on structure capacity during corrosion propagation time.

Reduction in the structure's time-dependent capacity either in the point correspondent to yield, or ultimate point is obvious in the studied structures. Figure (9) shows the capacity reduction occurred at different ages. It should also be mentioned that each of the time points are relative to the corrosion initiation time.

Due to the time-dependent effects of corrosion, displacement values correspondent to yield for corresponding time periods of 0 (pristine), 10, 20, 30, 40 and 50 years are 11.26, 10.25, 9.67, 9.17, 8.76 and 8.17 cm, respectively. These values are obtained from bilinear analysis of the pushover data.

After a 50-year life cycle, considering the corro-

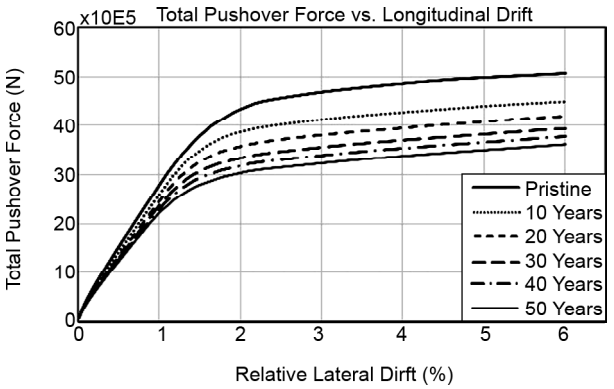

Figure 8. Time-dependent Pushover results.

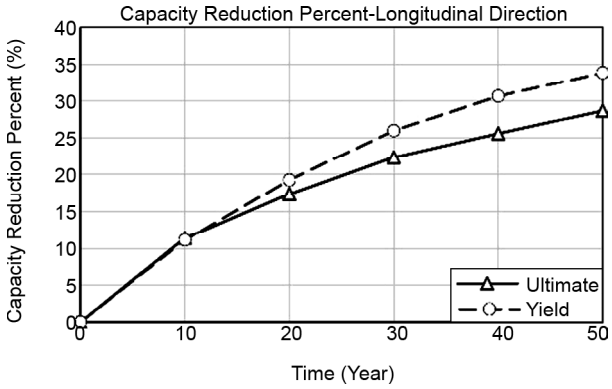

Figure 9. Bridges capacity reduction during the 50 yrs. lifetime.

Table 8. Total base shear values changes at various relative lateral drift.

Model Age (Year)*	Total Base Shear Reduction Percent Relative to Pristine Model					
	1%	2%	3%	4%	5%	6%
10 Years	6.85	10.67	12.05	12.17	11.81	11.42
20 Years	11.75	17.48	18.74	18.74	18.16	17.35
30 Years	15.00	22.96	24.12	23.94	23.31	22.32
40 Years	17.66	26.53	27.65	27.31	26.64	25.58
50 Years	20.41	29.90	30.98	30.52	29.80	28.70

*year: After corrosion initiation

sion effects, the displacement value correspondent to yield is reduced 27.44% relative to pristine structure.

The static pushover results give significant information about stiffness changes in the bridge resulting from corrosion effects. Figure (8) shows a decrease in the initial slope (stiffness) of the pushover curve as the level of corrosion damage increased according to the results. Due to the time-dependent effects of corrosion, the reductions in the initial stiffness of the bridge to pristine bridge for corresponding time periods of 10, 20, 30, 40 and 50 years are 4.77%, 8.36%, 10.75%, 12.84% and 13.73%, respectively.

Concrete cover by the 10th year, loses up to 55% and by the 20th year loses up to 95% of its primary strength gradually and after that time concrete cover does not exist actually. In all of the studied periods, reinforcement mechanical properties is gradually decreasing according to the trend presented in section 3, but the capacity reduction in the first 20 years while the concrete cover is diminishing due to corrosion effects, is more than the reduction in the third, fourth and fifth decades of the structure's life cycle. This indicates that the effect of loss of concrete cover on capacity reduction is more than the effect reduction of diameter and strength of reinforcement.

6. Nonlinear Time History Analyses

To determine the natural period of bridge, modal analysis is performed. Considering the effects of corrosion, the analysis results indicate that the natural period of bridge for corresponding time periods of 0 (pristine), 10, 20, 30, 40 and 50 years are 0.567, 0.594, 0.618, 0.623, 0.625 and 0.627 seconds, respectively.

To perform nonlinear time history analysis, a series including seven earthquake ground motions is selected and normalized to 0.3 g, 0.5 g and 0.75 g. In this study, to provide the ground motion records, PEER earthquake database is used [31]. The list of ground motion records used in this study is presented in Appendix A, where the earthquake magnitude (M) ranged from 6.5 to 7.4, the PGA ranged from 0.016 g to 0.537 g. To perform the analysis, the first mode Sa for 5% damping was selected. In this study, the effect of earthquake ground motions' vertical components was taken into account.

A series of nonlinear time history analyses is performed for six models correspondent to effects of corrosion at the time points of 0 (pristine), 10, 20, 30, 40 and 50 years. Due to the corrosion of reinforcing steel in the RC bridge, when the bridge is subjected to sample ground motion, the moment-curvature response of the central pier undergoes a significant reduction. This phenomenon is depicted in Figure (10), which shows a 19.84% increase in maximum curvature and a 27.17% reduction in maximum moment of a 50-year-old corroded column as compared to that of a pristine column. Other parameters during the time are illustrated in Table (9).

The results of analyses including response time-histories are recorded as forces and displacements. Deck drift ratio (DDR) is one of the reliable response measures among diverse response parameters derived from nonlinear time history analysis. The DDR is defined as the relative displacement of the deck centroid divided by the column height [32]. Hence, to put it in a nutshell, this paper presents the seismic response in terms of DDR only in both longitudinal and transverse directions. The mean of longitudinal and transverse DDR at different time steps is shown in Figure (11) for the different levels of earthquake intensity.

Table 9. Changes in results of time history analyses relative to pristine model (based on the percentage).

Model Age (year)*	Energy Dissipation	Initial Slope	Maximum Moment	Maximum Curvature
10 Years	7.32	18.66	8.86	6.12
20 Years	15.15	30.0	15.34	10.38
30 Years	19.53	36.76	20.63	13.83
40 Years	21.78	41.11	23.91	17.55
50 Years	23.68	45.14	27.17	19.84

*year: After corrosion initiation

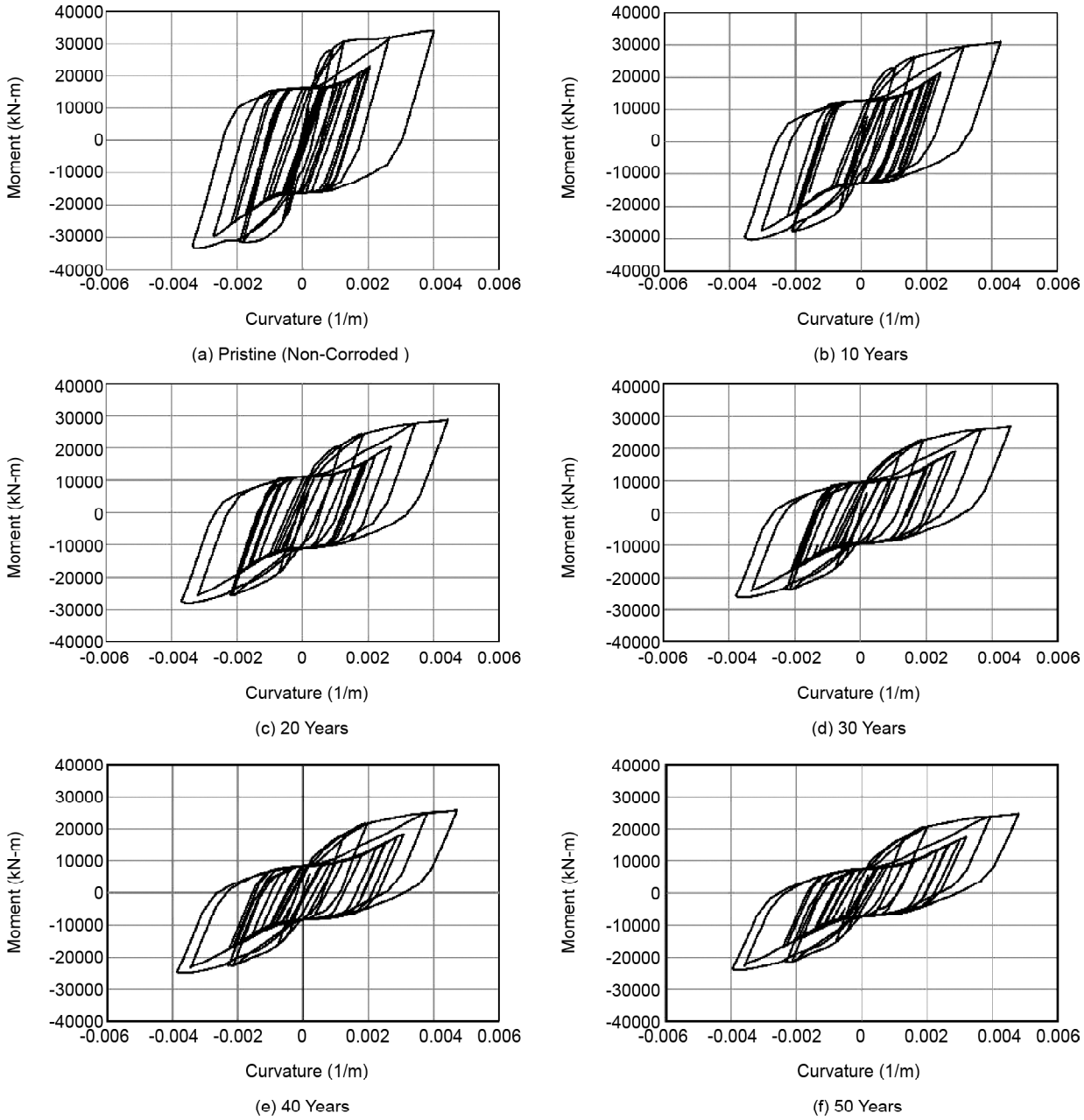

Figure 10. Moment-curvature response of the central column (sample ground motion).

Figure (11) clearly proves the gradual increase of mean deck drift ratios estimated during the 50-year period. The decrease in the slope seen after the 20th year, admitting the results of the static analyses, mentions the bigger effect of the removing concrete cover in comparison with degradation in the mechanical properties of the rebar in degradation resulted from corrosion. For example, in earthquakes with the intensity of 0.5 g, variations of this ratio in the 10th, 20th, 30th, 40th and 50th year after corrosion initiation, relative to the pristine structure in longitudinal direction are 14.35, 12.01, 8.20, 4.73 and 3.60, and in transversal direction are 21.36, 15.58, 9.32, 5.40, 4.25 percent.

Vulnerability level of the piers of the bridge considering corrosion according to curvature ductility was determined in both longitudinal and transverse direction.

To determine vulnerability level, column curvature ductility is taken here as the initial damage measure. The curvature ductility is defined as the ratio of maximum column curvature recorded from a non-linear time-history analysis to the column yield curvature achieved to moment-curvature analysis.

The curvature ductility values of the bridge calculated under the set of seven ground motions at

three levels of intensity (0.3g, 0.5g and 0.75g) and then compared with damage limit states. In this study, the damage limit states are assumed as shown in Table (10).

Comparing the frequency of occurrence of damage states within the set of seven ground motions at three levels of intensity (0.3 g, 0.5 g and 0.75 g) in analyses of the highway bridge, it is shown that non-damaged state probability in longitudinal direction is 52.38% and the probability of the complete damage is 9.52%. After some time with the structure aging and the corrosion effects propagating, in the 50 years old structure (after the corrosion initiation time) the probability of the

Table 10. damage limit states [4].

Damage State	Curvature Ductility
Slight	$1 \leq \mu_\varphi \leq 2$
Moderate	$2 \leq \mu_\varphi \leq 4$
Extensive	$4 \leq \mu_\varphi \leq 7$
Complete Damage	$7 \leq \mu_\varphi$

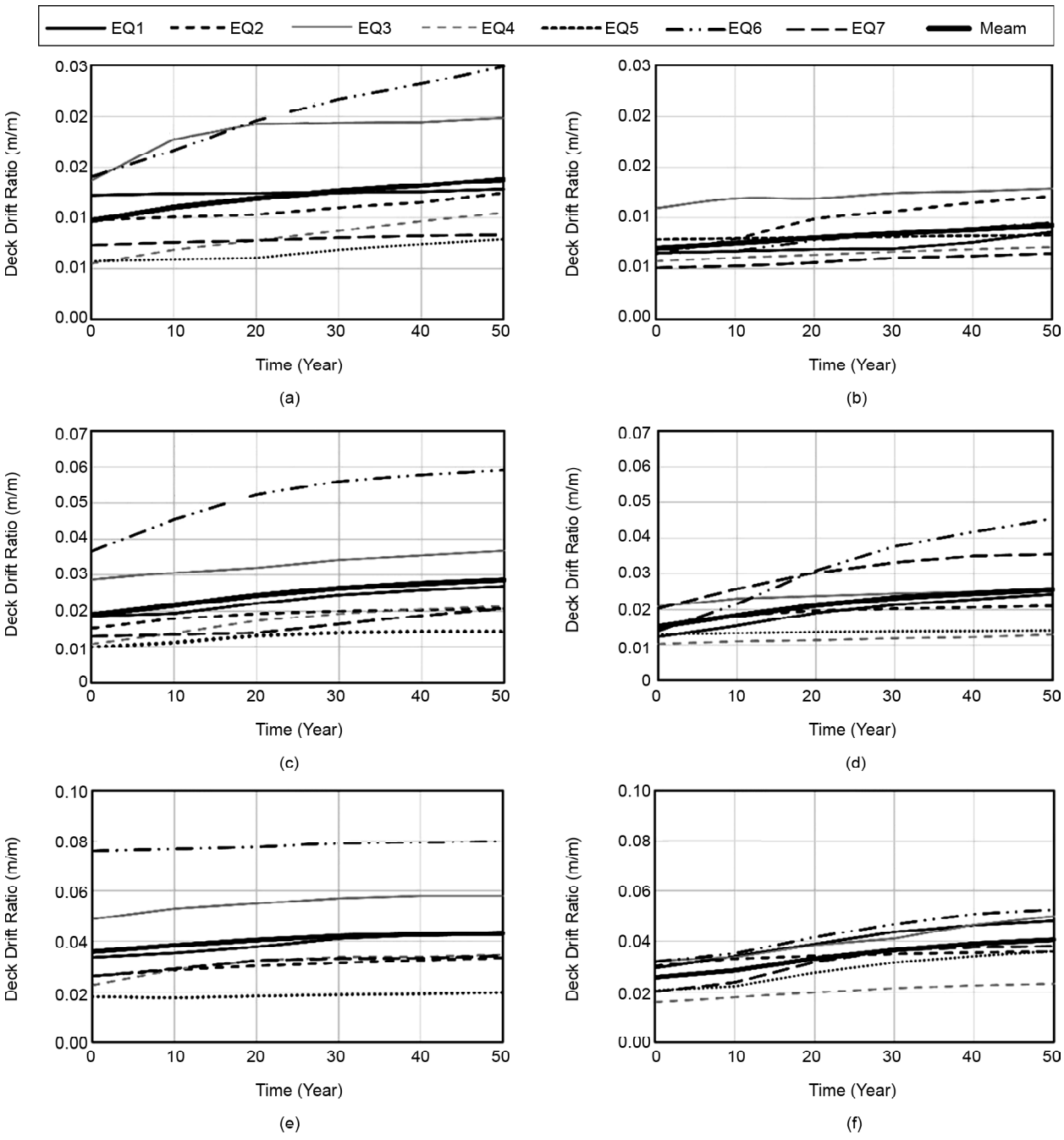

Figure 11. Change in mean values of DDR over 50 years after corrosion initiation time (on left, longitudinal direction; and on right, transverse direction): (a) for 0.3g; (b) for 0.5g; and (c) for 0.75g.

non-damaged state is reduced to 14.29% and the probability of fracture reaches 23.81%. In transverse direction, the probability of the non-damaged state is 52.38% and the probability of complete damage is 4.76%, which will be 38.1% for the 50-year aged corroded structure. Considering diverse corrosion effects and more earthquake intensity, it is proved that the bridge is more vulnerable in transverse direction than longitudinal direction.

7. Conclusions

In this study, the long-term corrosion process of a deteriorated typical RC highway bridge in Iran is analyzed as a function of time by using nonlinear static and dynamic analysis for seven earthquake ground motion records at three levels of intensity (0.3 g, 0.5 g and 0.75 g). The structural capacity and seismic performance level of the bridge was predicted as a function of the corrosion rate by taking into account three important corrosion effects considering experimental results obtained from Persian Gulf environmental conditions. The relationship between the corrosion rate and the structural effects caused by corrosion was explained.

As a result, it is determined that the removing of concrete cover on bottom of columns has a greater impact on the structural capacity of the RC bridge than decreasing the rebar mechanical parameters. Therefore, protecting concrete cover in such structures, which are exposed to corroding environments is the most important task in maintenance of these structures.

Comparing the frequency of occurrence of limit states according to curvature ductility, with the structure aging, corrosion effects propagating and earthquake magnitude increasing, it is observed that the probability of vulnerability of the piers of the bridge proposed in CODE No. 294 of the Management and Planning Organization of Iran (MPO), in transverse direction is bigger than longitudinal direction.

Bond strength reduction is disregarded in this study; however, if it is proved to have a major effect, it should be taken into account. In addition, other kinds of dynamic loading such as railroad vibrations can be investigated in probable extension to this study. Other loadings may lead to different results due to higher occurrence and different magnitude.

References

1. Vu, K. and Stewart, M.G. (2000) Structural reliability of concrete bridges including improved chloride-induced corrosion models. *Struct. Saf.*, **22**(4), 313-333.
2. Choe, D.E., Gardoni, P., Rosowsky, D., and Haukaas, T. (2008) Probabilistic capacity models and seismic fragility estimates for RC columns subject to corrosion. *Reliab. Eng. Syst. Saf.*, **93**(3), 383-393.
3. Choe, D.E., Gardoni, P., Rosowsky, D., and Haukaas, T. (2009) Seismic fragility estimates for reinforced concrete bridges subject to corrosion. *Struct. Saf.*, **31**(4), 275-283.
4. Choi, E., DesRoches, R., and Nielson, B. (2004) Seismic Fragility of typical bridges in moderate seismic zones. *Eng. Struct.*, **26**, 187-199.
5. Ghoddousi, P., Ganjian, E., Parhizkar, T., and Ramezanianpour, A.A. (1998) *Concrete Technology in the Environmental Conditions of Persian Gulf.* BHRC Publication, Tehran, Iran.
6. MPO No. 294 (2006) CODE No. 294, Management and Planning Organization of Iran, Tehran.
7. Tuutti, K. (1982) *Corrosion of Steel in Concrete. Cement and Concrete Research Institute*. Stockholm, Sweden.
8. Amleh, L., Lounis, Z., and Mirza, M.S. (2002) Reliability-based prediction of chloride ingress and reinforcement corrosion of aging concrete bridge decks - a case study investigation. *Proceedings of 6th International Conference on Short and Medium Span Bridges*, Vancouver, Canada, July-August.
9. ACI-365.1R-00 (2000) *Service Life Prediction-State of the Art Report*. American Concrete Institute (ACI), Farmington Hills, MI.
10. Ghosh, J. and Padgett, J. (2010) Aging Considerations in the development of time-dependent seismic fragility curves. *J. Struct. Eng.*, **136**(12), 1497-1511.
11. Ghods, P., Chini, M., Alizadeh, R., and Hosseini, M. (2005) The effect of different exposure conditions on the chloride diffusion into concrete in the Persian Gulf region. *Proceeding of*

International conference of ConMAT Conf., Vancouver, Canada, August.

12. Kashani, M., Crewe, A., and Alexander, N. (2012) Durability considerations in performance-based seismic assessment of deteriorated RC bridges. *Proceedings of 15th World Conference of Earthquake Engineering*, Lisbon, Portugal.

13. Bertolini, L., Elsener, B., Pedeferri, P., and Polder, R. (2004) *Corrosion of Steel in Concrete: Prevention, Diagnosis, Repair*. Wiley-VCH, Weinheim, Germany.

14. Al-Sulaimani, G.J., Kaleemullah, M., Basunbul, I.A., and Rasheeduzzafar (1990) Influence of corrosion and cracking on bond behavior and strength of reinforced concrete members. *ACI Struct. J.*, **87**(2), 220-231.

15. Ghandehari, M., Zulli, M., and Shah, S.P. (2000) Influence of corrosion on bond degradation in reinforced concrete. *Proceedings of 14th ASCE Engineering Mechanics Conference*, Austin, USA.

16. Alonso, C., Andrade, C., and Gonzalez, J.A. (1988) Relation between resistivity and corrosion rate of reinforcements in carbonated mortar made with several cement types. *Cement and Concrete Research*, **18**(5), 687-698.

17. Stewart, M.G. and Rosowsky, D. (1998) Structural safety and serviceability of concrete ridges subject to corrosion. *Journal of Infrastructure Systems*, **4**(4), 146-155.

18. Martinez, I. and Andrade, C. (2009) Examples of reinforcement corrosion monitoring by embedded sensors in concrete structures. *Cement & Concrete Composites*, **31**(8), 545-554.

19. Yalcyn, H. and Ergun, M. (1996) The prediction of corrosion rates of reinforcing steels in concrete. *Cement and Concrete Research*, **26**(10), 1593-1599.

20. Liu, Y. and Weyers, R.E. (1998) Modelling the time-to-corrosion cracking in chloride contaminated reinforced concrete structures. *ACI Materials Journal*, **95**(6), 675-681.

21. Duracrete (1998) *Probabilistic Performance Based Durability Design: Modelling of Degradation*. Document, D. P. BE95-1347/R4-5, the Netherlands.

22. Scott, A.N. (2004) *The Influence of Binder Type and Cracking on Reinforcing Steel Corrosion in Concrete*. Ph.D. Dissertation, University of Cape Town, Cape Town.

23. Du, Y.G., Clark, L.A., and Chan, A.H.C. (2005a) Residual capacity of corroded reinforcing bars. *Mag. Concr. Res.*, **57**(3), 135-147.

24. Du, Y.G., Clark, L.A., and Chan, A.H.C. (2005b) Effect of corrosion on ductility of reinforcing bars. *Mag. Concr. Res.*, **57**(7), 407- 419.

25. Li, C.Q., Melchers, R.E. and Zheng, J.J. (2006) Analytical model for corrosion-induced crack width in reinforced concrete structures. *ACI Structural Journal*, **103**(4), 479-487.

26. Zhong, J.Q., Gardoni, P., and Rosowsky, D. (2010) Stiffness degradation and time to cracking of cover concrete in reinforced concrete structures subject to corrosion. *Journal of Engineering Mechanics*, ASCE, **136**(2), 209-219.

27. Bazant, Z.P. and Planas, J. (1998) *Fracture and Size Effect in Concrete and Other Quasi-Brittle Materials*. CRC Press, Boca Raton, Florida and London.

28. OpenSees [Computer software] OpenSees Development Team, Pacific Earthquake Engineering Research Center, University of California, Berkeley, CA.

29. Karsan, I.D. and Jirsa, J.O. (1969) Behavior of Concrete under Compressive Loading. *Journal of the Structural Division, Proceeding of the American Society of Civil Engineers*, **95**(ST12), 2543-2563.

30. Mackie, K., and Stojadinovic, B. (2003) *Seismic Demands for Performance-Based Design of Bridges*. PEER Report 2003/16, Pacific Engineering Earthquake Research Center, University of California, Berkeley.

31. PEER Strong Motion Database (2013) http://peer.berkeley.edu/peer_ground_motion_database.

32. Alipour, A., Shafei, B., and Shinozuka, M. (2011) Performance evaluation of deteriorating highway bridges located in high seismic areas. *J. Bridge Eng.*, **16**(5), 597-611.

Appendix A

Appendix. List of ground motion records [31].

Event		M	Angle (˚)	PGA (g)	PGV (g)
EQ1	Landers	7.3	270	0.245	51.5
			360	0.152	29.7
			UP	0.136	12.9
EQ2	Kobe	6.9	0	0.141	15.6
			90	0.148	15.4
			UP	0.039	3.3
EQ3	Morgan Hill	6.5	90	0.051	5.8
			180	0.057	8.3
			UP	0.011	1.0
EQ4	Kocaeli, Turkey	7.4	0	0.224	50.3
			270	0.137	29.7
			UP	0.203	11.4
EQ5	Imperial Valley	6.5	140	0.519	46.9
			230	0.379	90.5
			UP	0.537	38.5
EQ6	Chi-Chi, Taiwan	7.3	N	0.419	118.4
			W	0.348	159.0
			V	0.241	110.5
EQ7	Loma Prieta	6.9	360	0.278	29.3
			270	0.197	37.5
			UP	0.090	10.2